Geochemical Perspectives Letters

Shock origin of the largest ureilitic microdiamond: structural observations and $\delta^{13}C$ value

O. Christ[1*#], A. Barbaro[1], G. Bragaggia[2], S. Gross[2], E. Thomassot[3], M.C. Domeneghetti[4], M. Alvaro[4], F.E. Brenker[5], F. Nestola[1,6]

https://doi.org/10.7185/geochemlet.2606

Abstract

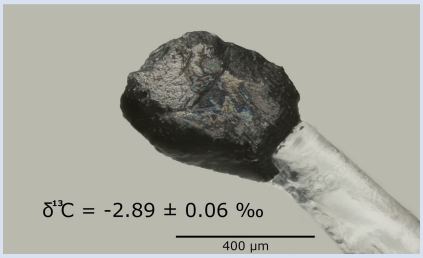

We report structural evidence for impact formed diaphite or stacking disorder in the largest known extraterrestrial microdiamond (>300 µm) from the highly shocked ureilite Northwest Africa 6871. Shock indicators within the microdiamond indicate a diamond formation model during the catastrophic disruption of the ureilite parent body, rather than deep static processes. After removal of associated graphite, large geometry secondary ion mass spectrometry yielded $\delta^{13}C = -2.89 \pm 0.06$ ‰, an intermediate value in the range of ureilitic $\delta^{13}C$ values. Combined with the Mg# of Northwest Africa 6871, the carbon isotopic signature shows that carbon was not affected by the impact which destroyed the ureilite parent body. Our findings therefore challenge the hypothesis that large ureilitic diamonds formed deep within their parent body and show that the carbon isotopes did not fractionate during diamond formation.

Received 4 August 2025 | Accepted 6 January 2026 | Published 13 February 2026

Introduction

Ever since their discovery, ureilitic diamonds have been intriguing scientific samples, and consensus on their formation process has not yet been reached as three major hypotheses remain debated within the scientific community: (i) formation inside a planetary body (Nabiei *et al.*, 2018), (ii) direct transformation from graphite to diamond upon shock (Nestola *et al.*, 2020) and (iii) crystal vapour deposition (Tomkins *et al.*, 2022). While the formation inside a planetary body has been favoured for large ureilitic diamonds (Miyahara *et al.* 2015, Nabiei *et al.*, 2018), the direct transformation from graphite to diamond during a shock event is still the most commonly accepted hypothesis (Nakamuta *et al.*, 2016, Nestola *et al.*, 2020; Barbaro *et al.*, 2021, 2023, 2025; Christ *et al.*, 2022; Rout *et al.*, 2023).

Ureilites are ultramafic carbon-rich achondrites, which originate from the ureilite parent body (UPB) (Goodrich, 1992). The history of the UPB is characterised by impact events in an early stage of our Solar System, which destroyed the partially differentiated UPB, producing one or more ureilite daughter bodies (Downes *et al.*, 2008). The shock formation hypothesis considers that during these impact events, high pressure and temperature regimes were reached which led to the direct transformation of graphite to diamond. Evidence for this direct transformation can be detected by X-ray diffraction (XRD) and transmission electron microscopy in the form of shock induced defects in both graphite and diamond (Nakamuta *et al.*, 2016, Németh *et al.*, 2022; Barbaro *et al.*, 2025).

Ureilitic diamond typically exhibits nanometric grain sizes; however, recent studies have revealed that nanometric diamond closely coexists with microdiamond (Nestola *et al.*, 2020; Barbaro *et al.*, 2021; Christ *et al.*, 2022), including a single crystal diamond measuring up to 100 µm in its longest dimension (Nestola *et al.*, 2020). Apart from that single crystal microdiamond, ureilitic microdiamonds are typically embedded in carbon aggregates with nanographite and nanodiamonds, making precise size estimation challenging. This can also be seen in the "unique large" diamond in the ureilite meteorite MS-170 reported by Miyahara *et al.* (2015), which consists of diamond aggregates with similar crystallographic orientations surrounded by graphite.

Carbon isotopes of both graphite and diamond in ureilites have been studied for a long time, and the combustion method is the most commonly used technique for analysing these phases (Grady *et al.*, 1985; Grady and Pillinger, 1986; Russell *et al.*, 1993; Smith *et al.*, 2001; Grady and Wright, 2003; Hudon *et al.*, 2004; Downes *et al.*, 2015; Barrat *et al.*, 2017). The combustion method,

1. Department of Geosciences, University of Padova, Via Gradenigo 6, 35131 Padova, Italy
2. Department of Chemical Sciences, Via Francesco Marzolo 1, 35131 Padova, Italy
3. University of Lorraine, University of Lorraine, ENSG 2 Rue du Doyen Marcel Roubault, BP 10162, 54505 Vandoeuvre-lès-Nancy Cedex, France
4. Department of Earth and Environmental Sciences, University of Pavia, Via A. Ferrata 1, 27100 Pavia, Italy
5. Schwiete Cosmochemistry Laboratory, Department of Geoscience, Goethe-University Frankfurt, Altenhöferallee 1, 60438 Frankfurt, Germany
6. Section Alessandro Guastoni, Museum of Nature and Humankind, University of Padova, Corso Garibaldi 39, 35121, Padova, Italy
Current address: Department of Earth and Environmental Sciences, University of Pavia, Via A. Ferrata 1, 27100 Pavia, Italy
* Corresponding author (e-mail: oliver.christ@unipv.it)

however, is a destructive method and combustion temperatures for graphite and diamond overlap between 600 °C and 900 °C (Grady *et al.*, 1985), making it challenging to assign specific $\delta^{13}C$ values to either phase. For example, the combustion method showed a primary release at 650 °C and, in some samples, a secondary minor release at approximately 900 °C and 1000 °C, both exhibiting nearly identical isotopic compositions (Downes *et al.*, 2015). The authors interpreted this secondary release as originating from either highly crystalline graphite or genetically related diamond, highlighting the difficulty in distinguishing between graphite and diamond. Further limitations of this method were pointed out by Fisenko *et al.* (2004), who noted that the combustion temperature is influenced by the available grain surface area and, consequently, the grain size, further complicating data comparisons. Generally, ureilitic $\delta^{13}C$ values form a continuous range from about −11 ‰ to about +7 ‰ with two peaks: one around −7 ‰ and one around −2 ‰, representing two carbon reservoirs which have not been fully mixed in the UPB (Barrat *et al.* 2017). Only four publications report carbon isotopic values for ureilitic diamond alone: pure diamond fractions/residues from the Novo Urei and Yamato 791538 meteorites (Vdovykin, 1970; Russell *et al.*, 1993; Fisenko *et al.*, 2004), and diamond FIB cuts from the Almahata Sitta MS-170 fragment (Miyahara *et al.*, 2015). The $\delta^{13}C$ values of the diamond fractions were reported to be −5.7 ‰ (Vdovykin, 1970), −5 ‰ and −1.8 ‰ (Russell *et al.*, 1993), and −2 ‰ (Fisenko *et al.*, 2004), while FIB cuts showed $\delta^{13}C$ values of −4.1 ‰ and −5.7 ‰ (Miyahara *et al.*, 2015). Additionally, the carbon isotopic composition of pure graphite has also been analysed (Storz *et al.*, 2021). Graphite from nineteen different ureilites was measured and showed a distinction between $\delta^{13}C$ values from graphite in coarse and fine grained ureilites. Graphite in coarse grained ureilites shows mean $\delta^{13}C$ values of −5.29 ‰, which are homogeneous within a single sample and are in good agreement with the hyperbolic relationship of $\delta^{13}C$ values with the Mg# of olivine cores reported by Barrat *et al.* (2017). In comparison, graphite in fine grained ureilites shows a heavier mean $\delta^{13}C$ of +1.94 ‰. However, values within one fine grained sample may vary. For example, the authors report $\delta^{13}C$ for graphite in the ureilite sample MS 20 which range between −9.29 ‰ and +4.09 ‰. The authors explained that fine grained ureilites are the result of impact processed, coarse grained ureilites and the difference in $\delta^{13}C$ with a smelting induced degassing scenario during impact on the UPB, which preferably consumed ^{12}C.

Here, we introduce a new, nearly non-destructive approach to investigate ureilitic diamond on the example of a large grain from Northwest Africa 6871 (NWA 6871). The sample was subjected to micro-XRD, and a two step cleaning procedure, which prepared the sample for isotopic characterisation using large geometry secondary ion mass spectrometry (LG-SIMS).

Sample and Methodology

This study was conducted on a diamond from the highly shocked ureilite NWA 6871. The highly shocked nature of NWA 6871 is evident in its apparently coarse grains, which are in fact olivine and pyroxene aggregates composed of numerous small grains, exhibiting a mosaicized texture. A detailed petrographic description of this ureilitic fragment can be found in Christ *et al.* (2022). The analysed grain was extracted from the bulk sample of NWA 6871 and mounted on a glass fibre (Fig. 1). In total, three large carbon-rich aggregates were extracted from the host ureilite and cleaned. However, reliable isotope measurements required the grains to have an almost flat surface, leaving only one grain suitable.

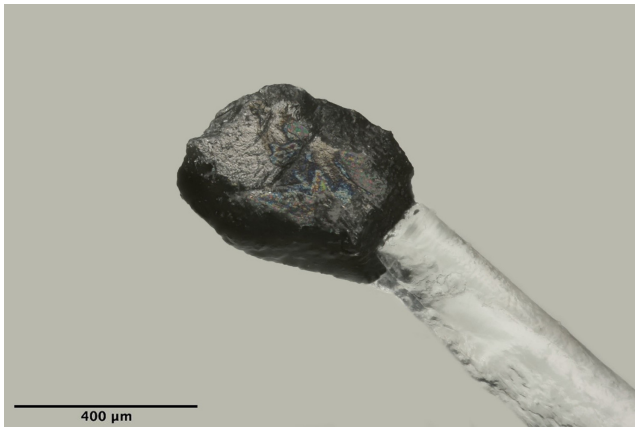

Figure 1 Microphotography of the diamond from NWA 6871, after the cleaning process, glued on top of a glass fibre (Microphotograph: Matteo Chinellato).

Analyses were performed using multiple micro-XRD measurements on a Rigaku Oxford Diffraction SuperNova single crystal diffractometer at the Department of Geosciences, University of Padua. The instrument features a 200K Dectris detector and operates with a microsource MoKα X-ray radiation at a wavelength of 0.71073 Å (with an X-ray beam diameter of 0.120 mm and a sample to detector distance of 69 mm). First measurements were performed over a range of 1–360° with a step size of 1° around the φ axis, and each frame was acquired for 100 seconds. After detecting unusually large single crystal diffraction spots for diamond, see Figure S-1, full data collections over the whole volume of the sample with 1262 frames over 19 runs and an exposure time of 20 seconds *per* frame were conducted.

After the initial micro-XRD characterisation, the diamond was placed in an ultrasound ethanol bath to remove the remaining matrix material. It was then remeasured to confirm the effectiveness of the cleaning process. Following this, a chemical cleaning procedure optimised by adapting an already reported subcritical hydrothermal process (Brown *et al.*, 2019) was performed at the Department of Chemical Sciences, University of Padua, to eliminate any remaining graphite. The process involved applying high temperature in a sealed vessel partially filled (12 % filling ratio) with a highly aggressive solution. Specifically, 18 mL of a solution containing HNO_3 (65 wt. %) and H_2SO_4 (96 wt. %), in a 1:2 molar ratio, was placed in a 150 mL PTFE vessel, which was then sealed tightly in a Berghof stainless steel Acid Digestion Bomb (12 % filling ratio) and heated at 250 °C for 48 hours. After cooling to room temperature, the diamond was recovered, washed several times with deionised water, and separated by centrifugation. A final micro-XRD measurement was conducted to ensure the successful removal of graphite.

Carbon isotope ratios were determined using large geometry secondary ion mass spectrometry (LG-SIMS) at the Centre de Recherches Pétrographiques et Géochimiques (CRPG) on a Cameca IMS-1280-HR multi-collection ion microprobe equipped with high sensitivity faraday cups following the high resolution procedure previously described in Gress *et al.* (2021). The analyses were achieved using a $^{133}Cs+$ primary beam (Gaussian mode), with a total acceleration voltage of 20 kV and a primary intensity of 4.2 ± 0.2 nA, corresponding to a spot size of ~15 µm. ^{12}C and ^{13}C were detected simultaneously on cross calibrated faraday cups (mass 12 on the central detector C and mass 13.003355 on H'2, using a 10^{11} Ω amplifier and a 10^{12} Ω

amplifier, respectively). Using such new generation collectors significantly improves the statistical errors (within spot uncertainties <0.2 ‰ 2σ; Bouden *et al.*, 2021). A collection of reference material previously characterised by IRMS after diamond combustion was used to precisely calibrate the instrumental mass fractionation. Both the samples and the standards were mounted in an indium ring in order to minimise degassing and improve the charge release as well as the counting stability.

Results

Optical microscopy revealed that the sample is up to 450 µm in length and has an irregular shape (Fig. 1). Micro-X-ray diffraction identified diffraction rings along with unusually large diffraction spots at *d* spacings of 2.06 Å, 1.26 Å, and 1.07 Å (Fig. 2a), indicating the presence of nanodiamond and single crystal diamond, respectively. Additionally, a characteristic shoulder in the diffractogram in Figure 2c (positioned at a *d* spacing of 2.16 Å) indicates the presence of stacking-disordered diamond or diaphite nanostructure (Németh *et al.*, 2022). Additional phases can be seen in peaks of graphite (*d* spacing of 3.34 Å), iron (*d* spacings of 1.17 Å and 1.43 Å), goethite (*d* spacing of 4.18 Å) and forsteritic olivine (*d* spacing of 2.46 Å). Compared to diamond, these phases show relatively low intensities. After the ultrasonic ethanol bath, the peaks for goethite (*d* spacing of 4.18 Å) and forsterite (*d* spacing of 2.46 Å) lost intensity (Fig. 2c).

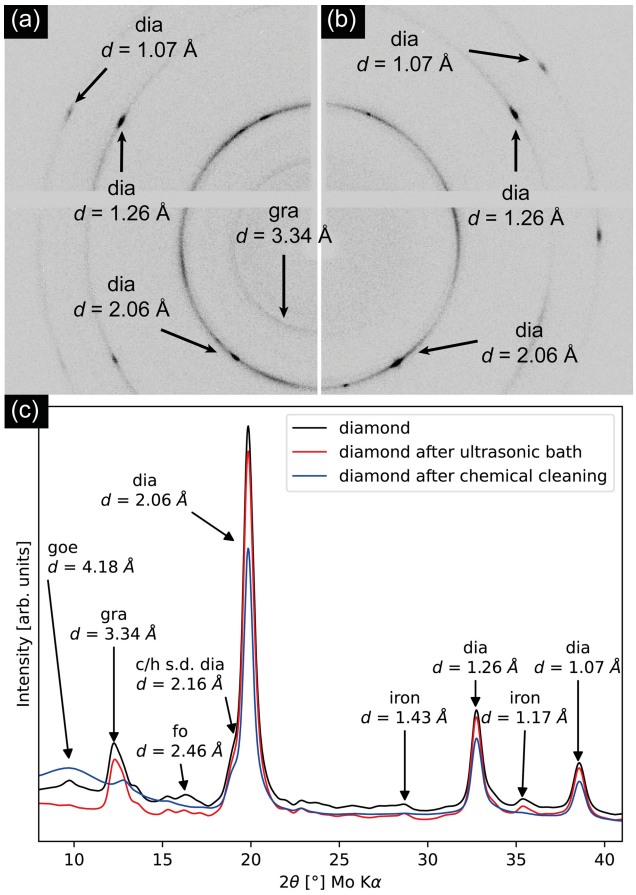

Figure 2 Documentation of the hydrothermal cleaning process. **(a)** Initial, diffraction image of the sample showing both rings and diffraction spots. Here, the large single crystal diffraction spots for diamond are most noteworthy. **(b)** Diffraction image of the diamond after the cleansing hydrothermal process. The graphite signal at *d* spacing 3.34 Å is lost as well as some polycrystalline material as shown by the lower intensities of the rings at *d* spacings 2.06 Å and 1.26 Å. **(c)** The initial diffractogram (black), the diffractogram after the ultrasonic bath (red), and the diffractogram after the chemical hydrothermal cleaning (blue). To provide better readability, not all small peaks have been labelled. Diffraction rings for iron and forsterite are not visible in **(a)** and **(b)** due to their low intensities and the contrast settings of the diffraction images. However, they can be seen in **(c).** Mineral abbreviations: dia = diamond, c/h s.d. dia = c/h stacking disordered diamond and/or diaphite, gra = graphite, goe = goethite, fo = forsterite, iron = metallic iron/Fe-Ni phases.

X-ray diffraction was repeated after the sample underwent hydrothermal treatment to remove graphite. The resulting diffractogram, shown in blue in Figure 2c, reveals the absence of the graphite diffraction peak at *d* spacing of 3.34 Å, confirming the successful removal of graphite. This is further supported by Figure 2a and b, where the graphite diffraction ring at 3.34 Å is no longer present in **(b).** After cleaning the sample, the diffractogram and diffraction image show only diamond, with minor forsterite and iron visible in the diffractogram. However, most of the sample consists solely of diamond, which is present in two distinct grain sizes. From the diffraction rings positioned at *d* spacings of 1.26 Å and 1.07 Å in the diffractograms, we calculated a crystallite size of approximately 5 nm using the Scherrer equation.

The $\delta^{13}C$ values are -2.74 ± 0.12 ‰, -2.62 ± 0.13 ‰, -2.74 ± 0.12 ‰ and -3.44 ± 0.11 ‰, yielding an average $\delta^{13}C_{mean}$ of -2.89 ± 0.06 ‰. Figure S-2 shows the locations of four LG-SIMS measurement points, which were collected on the 450 µm sized grain shown in Figure 1 (Dia 1 in Fig. S-3) while Table S-1 shows the results.

The results show that the cleaning method, which is typically used for larger gem diamonds, is capable of effectively cleaning smaller ureilitic diamonds. Further, the diamond studied here represents the largest extraterrestrial diamond found to date.

Discussion

The size of the diamond found in NWA 6871 is unprecedented and challenges the assumption that large ureilitic diamonds must have formed deep within the UPB through static processes, as the pressure-temperature conditions experienced by NWA 6871 are sufficiently high to induce shock driven diamond formation, even in the absence of metallic catalysts (Nakamuta *et al.*, 2016). The presence of shock indicators such as stacking faults in diamond and diaphite suggested by the XRD data, further supports this. Mineralogically, our sample closely resembles carbon aggregates from NWA 7983 (Nestola *et al.*, 2020), Kenna (Barbaro *et al.*, 2021), Yamato-74123 (Barbaro *et al.*, 2022), FRO 97013, 01088, 01012 (Barbaro *et al.*, 2023), and other diamonds from NWA 6871 (Christ *et al.*, 2022). What sets the sample of this study apart from other ureilitic diamonds, however, is its sheer size. While accurately determining the proportion of the single crystal region is challenging, the intensity contrast between the diffraction spots (*i.e.* the single crystal portion) and rings (*i.e.* nanocrystalline material) suggests that the single crystal domain is at least 300 µm in size. This estimate is based on XRD intensity measurements of similarly sized diamond single crystals obtained under identical experimental conditions.

LG-SIMS measurements yielded an average $\delta^{13}C$ of -2.89 ± 0.06 ‰. Comparing this to existing literature is challenging, as most available data come from conference abstracts without detailed methodology or the combustion method. All ureilitic diamonds exhibit intermediate $\delta^{13}C$ values, including the mean $\delta^{13}C$ value of -2.89 ± 0.06 ‰ from NWA 6871.

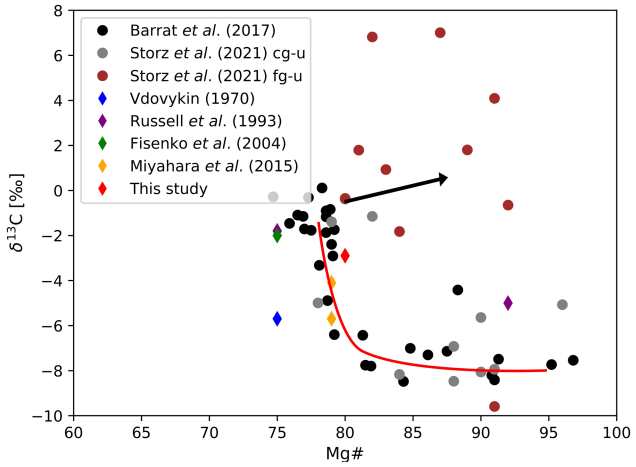

Figure 3 $\delta^{13}C$ *versus* Mg# plot. The black arrow indicates smelting. $\delta^{13}C$ data of diamonds and the Mg# of the host ureilites agrees very well with the hyperbolic relationship (red line) reported by Barrat *et al.* (2017). cg-u: coarse grained ureilites, fg-u: fine grained ureilites.

Discussing ureilitic $\delta^{13}C$ values requires considering also the olivine core composition (Mg#). Barrat *et al.* (2017) reported a hyperbolic relationship between the Mg# of olivine cores and the $\delta^{13}C$ and that, if this relationship is preserved, carbon has either remained isotopically unaffected or experienced only minor alteration. The $\delta^{13}C$ values of fine grained ureilites by Storz *et al.* (2021), however, do not follow the hyperbolic relationship. The authors interpreted these heavier values as ^{13}C enriched residues from an impact induced smelting process producing a CO gas, which mainly consisted of the lighter ^{12}C isotope. NWA 6871 has a forsterite composition of Fo_{80} (see Meteoritical Bulletin Nr. 100 entry). Figure 3 shows the data for NWA 6871 together with the other 4 available data sets in the $\delta^{13}C$ *vs.* Mg# plot including data from Barrat *et al.* (2017) and Storz *et al.* (2021). As can be observed, the hyperbolic relationship is preserved across all ureilitic diamonds, consistent with the findings of Maruoka *et al.* (2003), who reported that $\delta^{13}C$ differences between graphite and shock induced diamonds are minimal and, when detectable, insufficient to distinguish between shock and CVD formation processes. This underscores the importance of applying XRD analyses to identify potential crystallographic shock indicators. Combining XRD and LG-SIMS data, shock formed extraterrestrial diamonds preserve pristine carbon isotopic signatures and indicate that a large UPB is not necessary for the formation of large diamonds, which is in agreement with the findings of Downes *et al.* (2024). These authors have discussed that if diamonds were formed deep inside a Mercury- to Mars-sized UPB, as proposed by Nabiei *et al.* (2018), the host ureilite would show mineralogical evidence in the form of high pressure minerals as ringwoodite, majorite and diamond. Ringwoodite and majorite, however, are absent in NWA 6871.

Conclusions

The 450 μm diamond grain with a single crystal portion no smaller than about 300 μm from NWA 6871 is the largest ureilitic diamond reported to date. Micro-XRD analysis confirmed that ureilitic diamonds can be effectively cleaned of graphite using a method typically applied to larger gem diamonds, which enables nearly non-destructive carbon isotopic measurements solely on the ureilitic diamond while preserving the grain for further analyses. The $\delta^{13}C$ values of our 450 μm grain range from −2.62 ‰ to −3.44 ‰ (mean $\delta^{13}C = -2.89 \pm 0.06$ ‰, $n = 4$), which is consistent with the few $\delta^{13}C$ values reported for ureilitic diamonds. Generally, ureilitic diamonds exhibit intermediate carbon isotopic compositions in regard to the overall range of ureilitic $\delta^{13}C$ values. Carbon isotopic data alone, however, does not point towards any formation hypothesis but combining LG-SIMS with micro-XRD analyses it is reasonable to conclude that this large microdiamond formed directly from graphite during the shock event which destroyed the UPB, rather than deep inside a large UPB.

Acknowledgements

We would like to thank Francis McCubbin for editorial handling of our manuscript. Further we would like to thank Hilary Downes and Sami Mikhail as well as an anonymous reviewer for their constructive comments and suggestions, which strongly improved our manuscript. Lastly, we are grateful to Matteo Chinellato for providing his photo laboratory and capturing the image of our microdiamond and Nordine Bouden for his support during SIMS analyses. This study was carried out within the Space It Up project funded by the Italian Space Agency, ASI, and the Ministry of University and Research, MUR, under contract n. 2024-5-E.0-CUP n. I53D24000060005. AB has been supported by the Alexander Von Humboldt Foundation and by the DYNASTY project BARB_PNRR_RICERCA25_01 (ID SOE_20240000020). MA is supported by the Fondazione Cariplo grant agreement #2023-2431 and the PRINMIUR project n. 2022AL5MSN to M. Cremonesi. This work was supported by Programma Nazionale di Ricerche in Antartide 2018 [PNRA18 00247 – A to FN].

Editor: Francis McCubbin

Additional Information

Supplementary Information accompanies this letter at https://www.geochemicalperspectivesletters.org/article2606.

Cite this letter as: Christ, O., Barbaro, A., Bragaggia, G., Gross, S., Thomassot, E., Domeneghetti, M.C., Alvaro, M., Brenker, F.E., Nestola, F. (2026) Shock origin of the largest ureilitic microdiamond: structural observations and $\delta^{13}C$ value. *Geochem. Persp. Let.* 39, 12–16. https://doi.org/10.7185/geochemlet.2606

References

Barbaro, A., Domeneghetti, M.C., Litasov, K.D., Ferrière, L., Pittarello, L., Christ, O., Lorenzon, S., Alvaro, M., Nestola, F. (2021) Origin of micrometer-sized impact diamonds in ureilites by catalytic growth involving Fe-Ni-silicide: The example of Kenna meteorite. *Geochimica et Cosmochimica Acta* 309, 286–298. https://doi.org/10.1016/j.gca.2021.06.022

Barbaro, A., Nestola, F., Pittarello, L., Ferrière, L., Murri, M., Litasov, K.D., Christ, O., Alvaro, M., Domeneghetti, M.C. (2022) Characterization of carbon phases in Yamato 74123 ureilite to constrain the meteorite shock

history. *American Mineralogist* 107, 377–384. https://doi.org/10.2138/am-2021-7856

Barbaro, A., Domeneghetti, M.C., Fioretti, A. M., Alvaro, M., Nestola, F. (2023) Carbon polymorphs in Frontier Mountain ureilitic meteorites: a correlation with increasing the degree of shock. *Earth and Planetary Science Letter* 614, 118201. https://doi.org/10.1016/j.epsl.2023.118201

Barbaro, A., Nestola, F., Singerling, S.A., Nava, J., Brenker, F (2025) Nano-scale impact shock features of diamond and graphite in ureilites. *Carbon*, 120583 https://doi.org/10.1016/j.carbon.2025.120583

Barrat, J.-A., Sansjofre, P., Yamaguchi, A., Greenwood, R.C., Gillet, P. (2017) Carbon isotopic variation in ureilites: Evidence for an early, volatile-rich Inner Solar System. *Earth and Planetary Science Letters* 478, 143–149. https://doi.org/10.1016/j.epsl.2017.08.039

Bouden, N., Villeneuve, J., Marrocchi, Y., Deloule, E., Füri, E., Gurenko, A., Piani, L., Thomassot, E., Peres, P., Fernandes, F. (2021) Triple Oxygen Isotope Measurements by Multi-Collector Secondary Ion Mass Spectrometry. *Frontiers in Earth Science* 8, 601169. https://doi.org/10.3389/feart.2020.601169

Brown, K.J., Chartier, E., Sweet, E.M., Hopper, D.A., Bassett, L.C. (2019) Cleaning diamond surfaces using boiling acid treatment in a standard laboratory chemical hood. *Journal of Chemical Health & Safety* 26, 40–44. https://doi.org/10.1016/j.jchas.2019.06.001

Christ, O., Barbaro, A., Brenker, F.E., Nimis, P., Novella, D., Domeneghetti, M.C., Nestola, F. (2022) Shock degree and graphite geothermometry in ureilites NWA 6871 and NWA 3140. *Meteoritics & Planetary Science* 57, 1861–1878. https://doi.org/10.1111/maps.13907

Downes, H, Mittlefehldt, D.W., Kita, N.T., Valley, J.W. (2008) Evidence from polymict ureilite meteorites for a disrupted and re-accreted single ureilite parent asteroid gardened by several distinct impactors. *Geochimica et Cosmochimica Acta* 72, 4825–4844. https://doi.org/10.1016/j.gca.2008.06.028

Downes, H., Abernethy, F.A.J., Smith, C.L., Ross, A.J., Verchovsky, A.B., Grady, M.M., Jenniskens, P., Shaddad, M.H. (2015) Isotopic composition of carbon and nitrogen in ureilitic fragments of the Almahata Sitta meteorite. *Meteoritics & Planetary Science* 50, 255–272. https://doi.org/10.1111/maps.12413

Downes, H., Mittlefehldt, D.W., Ross, A.J., Lee, C.-T. (2024) Extra-terrestrial mantle samples: Rare Earth Element variations and evidence for melt metasomatism in ureilite meteorites. *Lithos* 486–487, 107775. https://doi.org/10.1016/j.lithos.2024.107775

Fisenko, A.V., Verchovsky, A.B., Semjonova, L.F., Pillinger, C.T. (2004) Carbon, Nitrogen, and Noble Gases in the Diamond Fractions of the Novo Urei Ureilite. *Solar System Research* 38, 383–393. https://doi.org/10.1023/B:SOLS.0000043814.61956.4c

Goodrich, C.A. (1992) Ureilites: A critical review. *Meteoritics* 27, 327–352. https://doi.org/10.1111/j.1945-5100.1992.tb00215.x

Grady, M.M., Pillinger, C.T. (1986) The ALHA 82130 ureilite: Its light element stable isotope composition and relationship to other ureilites. *Abstracts and Program for the 49th Annual Meeting of the Meteoritical Society*. https://adsabs.harvard.edu/full/1986LPICo.600E.196G

Grady, M.M., Wright, I.P., Swart, P.K., Pillinger, C.T. (1985) The carbon and nitrogen isotopic composition of ureilites: Implications for their genesis. *Geochimica et Cosmochimica Acta* 49, 903–915. https://doi.org/10.1016/0016-7037(85)90306-0

Grady, M.M., Wright, I.P. (2003) Elemental and isotopic abundances of carbon and nitrogen in meteorites. *Space Science Reviews* 106, 231–248. https://doi.org/10.1023/A:1024645906350

Gress, M.U., Timmerman, S., Chinn, I.L., Koornneef, J.M., Thomassot, E., van der Walk, E.A.S., van Zuilen, K., Bouden, N., Davies, G.R. (2021) Two billion years of episodic and simultaneous websteritic and eclogitic diamond formation beneath the Orapa kimberlite cluster, Botswana. *Contributions to Mineralogy and Petrology* 176, 54. https://doi.org/10.1007/s00410-021-01802-8

Hudon, P., Romanek, C., Paddock, L., Mittlefehldt, D.W. (2004) *Evolution of the Ureilite Parent Body. 35th Lunar and Planetary Science Conference, 2075*.

Maruoka, T., Koeberl, C., Matsuda, J.I., Syono, Y. (2003) Carbon isotope fractionation between graphite and diamond during shock experiments. *Meteoritics & Planetary Science* 38, 1255–1262. https://doi.org/10.1111/j.1945-5100.2003.tb00311.x

Miyahara, M., Ohtani E., El Goresy, A., Lin, Y., Feng, L., Zhang, J.-C., Gillet, P., Nagase, T., Muto, J., Nishijima, M. (2015) Unique large diamonds in a ureilite from Almahata Sitta 2008 TC3 asteroid. *Geochimica et Cosmochimica Acta* 163, 14–26. https://doi.org/10.1016/j.gca.2015.04.035

Nabiei, F., Badro, J., Dennenwaldt, T., Oveisi, E., Cantoni, M., Hébert, C., El Goresy, A., Barrat, J.-A., Gillet, P. (2018) A large planetary body inferred from diamond inclusions in a ureilite meteorite. *Nature Communications* 9, 1–6. https://doi.org/10.1038/s41467-018-03808-6

Nakamuta, Y., Kitajima, F., Shimada, K. (2016) In situ observation, X-ray diffraction and Raman analyses of carbon minerals in ureilites: Origin and formation mechanisms of diamond in ureilites. *Journal of Mineralogical and Petrological Sciences* 111, 252—269. https://doi.org/10.2465/jmps.150906

Németh, P., Lancaster, H.J., Salzmann, C.G., McColl, K., Fogarassy, Z., Garvie, L.A.J., Illés, L., Pécz, B., Murri, M., Corà, F., Smith, R.L., Mezouar, M., Howard, C.A., McMillan, P.F. (2022) Shock-formed carbon materials with intergrown sp^3 - and sp^2-bonded nanostructured units. *Proceedings of the National Academy of Sciences* 119. https://doi.org/10.1073/pnas.2203672119

Nestola, F., Goodrich, C.A., Morana, M., Barbaro, A., Jakubek, R.S., Christ, O., Brenker, F.E., Domeneghetti, M.C., Dalconi, M.C., Alvaro, M., Fioretti, A.M., Litasov, K.D., Fries, M.D., Leoni, M., Casati, N.P.M., Jenniskens, P., Shaddad, M.H. (2020) Impact shock origin of diamonds in ureilite meteorites. *Proceedings of the National Academy of Sciences* 117, 25310–25318. https://doi.org/10.1073/pnas.1919067117

Rout, S.S., Storz, J., Davydok, A., Bischoff, A., John, T., Krywka, C., Ritter, M. (2023) Formation of diamond and lonsdaleite in ureilites by impact shock processing of graphite. *Meteoritics & Planetary Science* 58, 1469–1494. https://doi.org/10.1111/maps.14082

Russell, S.S., Arden, J.W., Franchi, I.A., Pillinger, C.T. (1993) A carbon and nitrogen isotope study of carbonaceous vein material in ureilite meteorites. *Lunar and Planetary Institute, 24th Lunar and Planetary Science Conference, part 3*, 1221–1222. https://adsabs.harvard.edu/full/1993LPI....24.1221R

Smith, C.L., Franchi, I.A., Wright, I.P., Grady, M.M., Pillinger, C.T. (2001) New Data on Carbon Isotopic Compositions of Some Ureilites. *Lunar and Planetary Institute, 32nd Lunar and Planetary Science Conference Abstract #1878*. http://www.lpi.usra.edu/meetings/lpsc2001/pdf/1878.pdf

Storz, J., Ludwig, T., Bischoff, A., Schwarz, W.H., Trieloff, M. (2021) Graphite in ureilites, enstatite chondrites, and unique clasts in ordinary chondrites – Insights from the carbon-isotope composition. *Geochimica et Cosmochimica Acta* 307, 86–104. https://doi.org/10.1016/j.gca.2021.05.028

Tomkins, A.G., Wilson, N.C., McRae, C., Salek, A., Field, M.R., Brand, H.E.A., Langendam, A.D., Stephen, N.R., Torpy, A., Pintér, Z., Jennings, L.A., McCulloch, D.G. (2022) Sequential Lonsdaleite to Diamond Formation in Ureilite Meteorites via In Situ Chemical Fluid/Vapor Deposition. *Proceedings of the National Academy of Sciences* 119, 1–8. https://doi.org/10.1073/pnas.2208814119

Vdovykin, G.P. (1970) Ureilites. *Space Science Reviews* 10, 483–510. https://doi.org/10.1007/BF00172536